ACADEMIC PRESS

Available online at www.sciencedirect.com
SCIENCE DIRECT®

Journal of Catalysis 214 (2003) 179–190

JOURNAL OF CATALYSIS

www.elsevier.com/locate/jcat

Selective catalytic reduction of NO_x by methane over Co-H-MFI and Co-H-FER zeolite catalysts: characterisation and catalytic activity

C. Resini,[a,b] T. Montanari,[a,b] L. Nappi,[a,c] G. Bagnasco,[a,c] M. Turco,[a,c] G. Busca,[a,c,*] F. Bregani,[d] M. Notaro,[d] and G. Rocchini [d]

[a] *Consorzio INSTM, via Benedetto Varchi, 59, 50132 Florence, Italy*
[b] *Dipartimento di Ingegneria Chimica e di Processo, Università degli Studi di Genoa, Genova, Italy*
[c] *Dipartimento di Ingegneria Chimica, Università "Federico II" di Napoli, Naples, Italy*
[d] *BU Processi per la Generazione, CESI S.p.A., via Reggio Emilia, 39, 20090 Segrate (MI), Italy*

Received 11 July 2002; revised 11 November 2002; accepted 19 November 2002

Abstract

Co-H-MFI and Co-H-FER were studied as catalysts for NO reduction with methane, under diluted conditions. Catalyst bulk and surface structure was characterised by chemical analysis, XRD, TG-DTA, SEM micrographs, IR studies, UV–vis spectroscopy, ammonia TPD, and TPR. Only the features due to zeolitic frameworks were observed. The UV–vis spectra showed that, after outgassing, Co ions are mainly present as Co^{2+}. FT-IR detected residual bridging hydroxyl and silanol groups in spite of the apparent over-exchange, deduced from the chemical analysis. Co ions gave rise to Lewis acid sites of medium strength, evidenced through in situ analysis of the adsorption of a basic probe molecule. NH_3-TPD measurements fully confirmed these results. TPR measurements detected easily reducible and oxidizable Co species, possibly related to nanosized Co oxide phases, together with hardly reducible Co^{2+} ions. Catalytic tests highlighted the Co-H-FER and Co-H-MFI activity, both in NO-selective catalytic reduction by methane and in NO oxidation to NO_2, the latter being the predominant reaction at low temperatures. Some mechanistic features of the CH_4-SCR reaction are discussed.

Keywords: CH_4-SCR; NO_x reduction; Co-exchanged zeolites; Co-H-FER; Co-H-MFI; Co-H-ZSM5; Acidity characterisation; IR spectroscopy; Nitrile adsorption; UV–vis spectroscopy

1. Introduction

The removal of nitrogen oxides from flue gases of thermal power plants is currently carried out with the so-called NH_3-SCR technology, i.e., the selective catalytic reduction of NO by ammonia [1,2] over V_2O_5–WO_3/TiO_2 or V_2O_5–MoO_3/TiO_2 catalysts through the overall reaction

$$4NH_3 + 4NO + O_2 \rightarrow 4N_2 + 6H_2O. \quad (1)$$

The need to store ammonia is one of the main drawbacks of this technology when applied to power plants. Additionally, the possible formation of ammonium sulphates due to reaction of SO_2, oxygen, water, and ammonia and the danger of ammonia leakage may also limit the conditions for application of such process.

A valid alternative process for denitrification of exhaust gases from power plants (as NO decomposition is not yet applicable) implies the use of methane as the reducing agent.

The likely overall reaction for the CH_4-SCR technique is [3]

$$CH_4 + 2NO + O_2 \rightarrow N_2 + CO_2 + 2H_2O. \quad (2)$$

The possibility of reducing NO with hydrocarbons such as olefins and higher alkanes was first proposed in 1990 by Held et al. [4] and by Iwamoto et al. [5] and Cu-MFI catalysts were found to be particularly active. However, these catalysts are poorly effective with methane as reductant. Methane as a reductant is, however, the preferred choice for NO_x removal from flue gases because it is already present in methane-fueled power plants. Co-containing zeolites, such as Co-MFI and Co-FER, were found by Armor [6] to be particularly active in CH_4-SCR in the presence of oxygen. These catalysts work in the temperature range from 573

* Corresponding author.
E-mail address: Guido.Busca@unige.it (G. Busca).

0021-9517/03/$ – see front matter
doi:10.1016/S0021-9517(02)00153-7

to 773 K and at space velocities that allow application in high-dust configurations.

Co^{2+} ions exchanged in a zeolitic matrix are considered to be the active sites [7,8]. The reaction mechanism for these catalysts was also investigated [9–11]. The activity of the catalysts is significantly inhibited by steam [12] but this effect can be limited, for instance, by mixing the zeolite catalysts with metal oxides such as manganese oxide [13].

The main drawback of these catalysts is their hydrothermal instability due to dealumination and loss of the active phase [14]. It has been reported that deactivation by dealumination is slower for small than for large crystal size Co-MFI samples [15]. Moreover, these catalysts are SO_x sensitive, although that effect also can be limited by modifying the zeolite composition [16].

To improve such catalysts' stability, addition of other components to Co-zeolites has been attempted [17,18]. In spite of many efforts, the durability problems of transition-metal-containing zeolites have not yet been resolved. On the other hand, several more questions have been opened about these catalysts. The reason these materials are more active than mixed oxides containing the same metal oxides is not yet fully understood.

Recently, it has been proposed that cooperation between transition metal cations and Brønsted acid sites can occur upon CH_4-SCR. According to Yan et al. [19], Co cations act in the oxidation of NO to NO_2 while Brønsted acid sites act in the true reduction step by methane. In contrast, Kauchy et al. [8] suggest that Brønsted sites enhance the activity in oxidising NO to NO_2.

In the present work Co-exchanged MFI and ferrierite (FER) zeolites obtained from NH_4^+-zeolites were studied for CH_4-SCR. The study was aimed to obtain information on the nature of active sites and to investigate the role of protonic sites. To gain this purpose several characterisation techniques were employed that can give complementary results, such as FT-IR, UV–vis diffuse reflectance, NH_3-TPD and TPR.

2. Experiments and methods

2.1. Catalyst preparation

NH_4-MFI ($SiO_2/Al_2O_3 = 50$, $S = 425\ m^2\,g^{-1}$) and NH_4-FER ($SiO_2/Al_2O_3 = 55$, $S = 480\ m^2\,g^{-1}$) supplied by Zeolyst were used as starting materials. NH_4-zeolite powders were contacted with a 0.02 M $(CH_3COO)_2Co \cdot 4H_2O$ aqueous solution (10 g powder for 1 L solution) under stirring at a constant temperature of 353 K for 24 h. The resulting mixture was filtered and washed three times with double-distilled water. After centrifugation, powders were dried at 353 K for 10 h and calcined at 823 K for 4 h.

2.2. Catalyst characterisation

Chemical analysis of the catalysts was performed by atomic absorption spectroscopy.

Surface area and pore size distribution measurements were performed by N_2 adsorption at 77 K using the Dubinin–Radushkevich method for the calculation of the surface area and the Horvath method for the pore size distribution.

XRD analysis was performed with a Philips PW1710/1729 diffractometer (Cu-K_α radiation). The cell parameters were calculated using the ASPO program. The crystal size was calculated using the Sherrer formula and considering the most intense XRD peaks. TG-DTA analyses were effected with a Setaram T92 analyser.

Scanning electron microscope (SEM) observations were made using a model Cambridge Leo microscope equipped with a model Link Isis microanalysis system of the dispersion energy type. All images were obtained with secondary electrons.

Diffuse reflectance spectra (DR-UV–vis–NIR) of pure self-supported sample powder disks were recorded by a Jasco V-570 apparatus in the range 50,000–4000 cm^{-1} at room temperature (rt) in air, and after dehydration at 773 K for 5 h by outgassing through a conventional gas manipulation/outgassing ramp connected to a quartz cell.

The IR spectra were recorded on a Nicolet Protégé 460 Fourier transform instrument. The surface characterisation was performed using pressed disks of pure NH_4-zeolite and Co-H-zeolite powders (15 mg, 2 cm diameter), activated by outgassing at 773 K in the IR cell. A conventional manipulation/outgassing ramp connected to the IR cell was used. Spectra were collected after the activation procedure and after adsorption of acetonitrile (AN), supplied by Aldrich and distilled under vacuum prior to use. The adsorption procedure involves contact of the activated sample disk with vapours at rt and at a pressure of 15 Torr, and outgassing in steps from rt to higher temperatures.

Temperature programmed desorption of ammonia (NH_3-TPD) was performed in a flow laboratory plant equipped with a thermal conductivity detector (TCD). The sample, treated in He flow at 773 K, was saturated with a 1% NH_3/He mixture at rt and purged with He at rt; then NH_3-TPD was effected by heating in He flow at a rate of 10 $K\,min^{-1}$. A KOH trap was placed between the sample and the TCD in order to avoid interference by H_2O.

Temperature programmed reduction (TPR) tests were performed by a Micromeritics TPD/TPR 2900 instrument. The sample was heated at a rate of 10 $K\,min^{-1}$ up to 1073 K under a gas flow (22 $mL\,min^{-1}$) of 2% H_2 in Ar. In such a way the catalyst samples were reduced and the amount of consumed H_2 was measured by a TCD detector. The H_2O produced in the reduction was removed by a cold trap (melting isopropanol) placed before the TCD.

2.3. Catalytic activity measurements

Catalytic tests were performed in a flow laboratory plant equipped with a fixed bed reactor operating at atmospheric pressure. The operation conditions were: reacting mixture composition, NO = 1500 ppm, CH_4 = 1500 ppm, O_2 = 25,000 ppm, He balance; T = 523–773 K; GHSV = 30,000–60,000 h^{-1}. Grain dimensions of the catalysts were 150–212 μm. The analyses of NO, NO_2, and N_2O was performed by an ABB URAS 14 continuous spectrophotometer analyser equipped with a NO_2 converter. CH_4, N_2, CO, and CO_2 concentrations were measured by an HP 5890 gas chromatograph with a TCD detector and a 5A-Porapak Q double-packed molecular sieve column.

3. Results

3.1. Structural and morphological catalyst characterisation

The SEM micrographs of the exchanged samples are reported in Fig. 1. The crystal shape is the same as for the original ammonium zeolites, showing that for the MFI sample the particles are nearly spherical with an apparent diameter of 100–250 nm. For FER the particles are clearly sheet-like, nearly 50 nm thick. The XRD patterns of both unexchanged and exchanged samples correspond to those of the related pure zeolite, without any other detectable phase. The crystal sizes, calculated by the Sherrer method on the most intense peaks, are nearly 50 nm for FER and 25 nm for MFI.

FT-IR skeletal spectra do not provide any evidence for a significant perturbation of the zeolite framework spectra due to the ion-exchange process. On the other hand, both Co-zeolites show, in the far-IR region, an additional weak band at 250 cm^{-1} which could be assigned to the in-cavity cobalt–oxygen stretching, as previously reported for other metal-exchanged zeolites [20].

The TG-DTA analyses of the parent ammonium zeolites and of Co-exchanged samples agree with those expected for these samples, as regards water release and ammonium decomposition. In all cases, water and ammonia desorption is complete around 773 K. For Co-MFI a further small weight loss, possibly associated with decomposition of Co oxide species, occurs around 973 K. Above that temperature slow weight losses are observed for all the samples, possibly due to dehydration of structural OHs, with corresponding zeolitic structures decomposition.

The results of chemical analysis and textural characterisation of the catalysts are reported in Table 1. It can be observed that the Si/Al ratios experimentally evaluated are very close to the theoretical ones. The cobalt content of both samples is higher than that corresponding to complete ion exchange capacity evaluated from the Si/Al ratio. Moreover it can be observed that the Co-exchange procedure and following calcination at 823 K do not modify the surface areas of the parent zeolites.

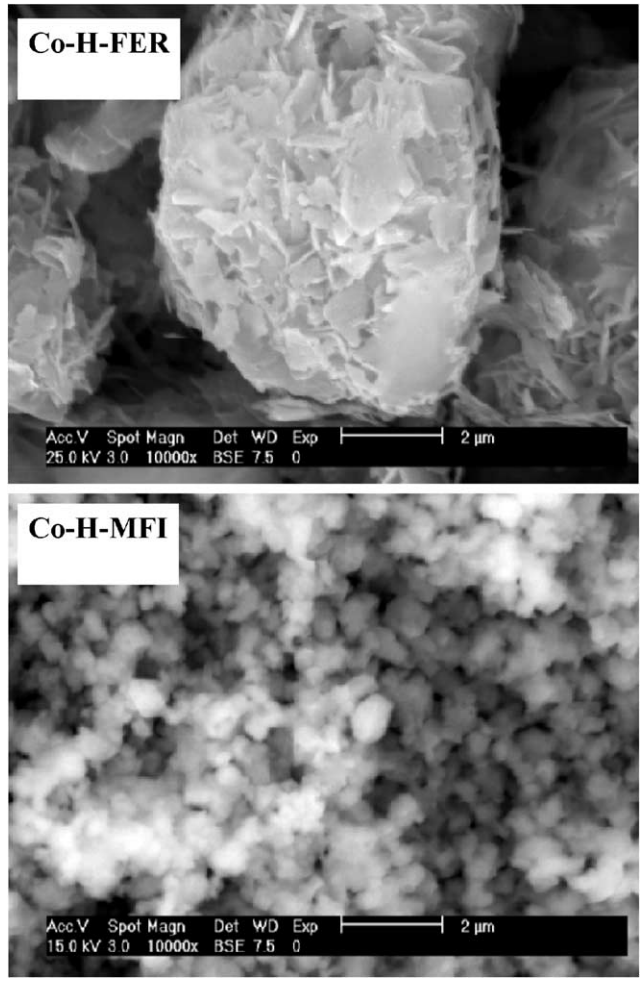

Fig. 1. SEM micrographs of Co-exchanged zeolites.

3.2. UV–vis spectroscopic characterisation

The DR-UV–vis spectra of both ammonium and Co-zeolites, recorded under ambient conditions, are reported in Fig. 2. The UV–vis spectrum of the most stable cobalt oxide, Co_3O_4 (supplied by Carlo Erba, S = 15 $m^2\,g^{-1}$), is reported too. Absorptions due to Co^{n+} can be clearly seen in the spectra of cobalt-containing zeolites as a very strong broad band centred near 26,000 cm^{-1} and a shoulder near 19,000 cm^{-1}. In the case of Co-containing MFI significant

Table 1
Textural properties and analytical data of Co-zeolites

	Si/Al exp.	Si/Al theor.	Co wt% exp.	Co/Al exp.	S $m^2\,g^{-1}$	V_{MP} $cm^3\,g^{-1}$	D_P Å
Co-H-FER	28.51	27.5	2.21	0.73	451	0.160	5.3
Co-H-MFI	28.31	25.0	1.71	0.55	466	0.159	5.5

S = specific surface area; V_{MP} = micropore volume; D_P = average pore diameter.

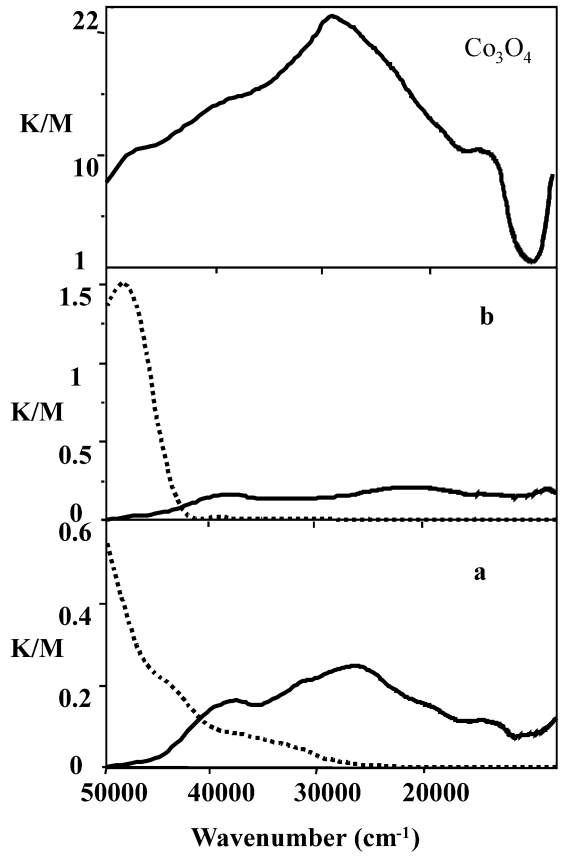

Fig. 2. UV–vis spectra of H-zeolites (···) and Co-exchanged zeolites (—) at rt in air: (a) MFI, (b) FER. The spectrum of Co_3O_4 is reported too.

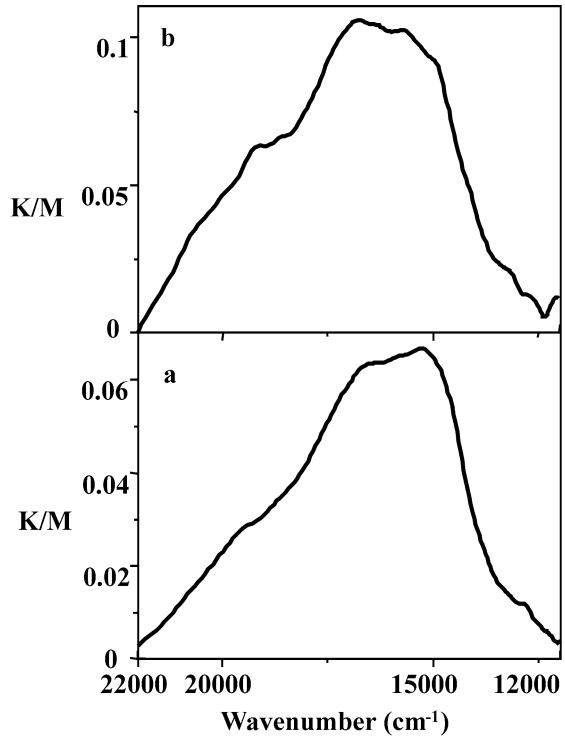

Fig. 3. UV–vis spectra of Co-MFI (a) and Co-FER (b) after outgassing at 773 K for 5 h.

absorption is also evident in the region between 20,000 and 10,000 cm^{-1} with a further maximum near 14,000 cm^{-1}. The spectrum of Co-H-FER does not give any evidence for the presence of massive Co_3O_4. On the contrary, the spectrum of Co-H-MFI in these conditions is similar to that of Co_3O_4. In Fig. 3 the spectra of cobalt-exchanged FER and MFI recorded after evacuation at 773 K for 5 h are reported. The very strong and broad absorption observed in the ambient conditions spectra does not appear any longer, showing that activation under vacuum causes a change in the oxidation and/or coordination state of Co^{n+} ions. The very high-energy region (above 40,000 cm^{-1}) is unavailable in the spectrum because our vacuum cell causes strong noise there. Weak absorptions are found which can be interpreted as a triplet near 19,000 cm^{-1}, near 17,000 cm^{-1} and near 15,000 cm^{-1}. No other absorption occurs in the range 40,000–22,000 cm^{-1}. The spectrum we observe is close to those reported and deeply discussed by Kauchy et al. for Co-FER [21] and by Dedechek et al. for Co-MFI [22]. These authors assigned the spectra to Co^{2+} in exchanged positions in the zeolite cavities. Three families of Co^{2+} ions in the zeolite cavities would exist, according to these authors. In one of the sites Co^{2+} is coordinated to four oxygen atoms arranged in a rectangle which is situated in the wall of the straight channel of MFI and in that of the main channel of FER. Co^{2+} in this site is responsible for a single band at 14,800–15,000 cm^{-1}. A second family of absorption components is related to Co^{2+} sitting in a deformed six-ring made of six framework oxygen atoms allocated at the intersection of the straight and the sinusoidal channels of MFI and in the eight-ring channel of FER. This species is considered to be responsible for four absorption components in the range 15,900–21,000 cm^{-1} with the main maximum near 17,000 cm^{-1}. According to these authors, this kind of site is that predominately occupied at all Co loadings. The last site type is a boat-shaped site that can be found in the wall of the sinusoidal channel of MFI and in the eight-ring channel of FER. The exact geometry and the number of coordinated oxygen atoms are still unknown for the investigated materials; it is occupied only at high Co loadings and gives rise to two absorption components in the range 20,000–22,000 cm^{-1}.

To check the picture given by Kauchky et al. [21] and by Dedechek et al. [22], we further investigated, under the same conditions, the UV spectroscopy of other Co-containing samples, such as Co–silica–aluminas. We find on these samples spectra quite similar to those on Co-MFI and Co-FER, with absorption again in the region 22,000–14,000 cm^{-1}. So we can suppose that Co species located at the external zeolite surface (which likely exist, as deduced from IR spectra, see below, and are likely similar to those of Co–silica–alumina) cannot be distinguished from the internal Co species. The presence of these species has not been considered in previous studies [21,22]. In agreement with Dedechek et al. absorption bands characteristic neither of hydrated Co^{2+}

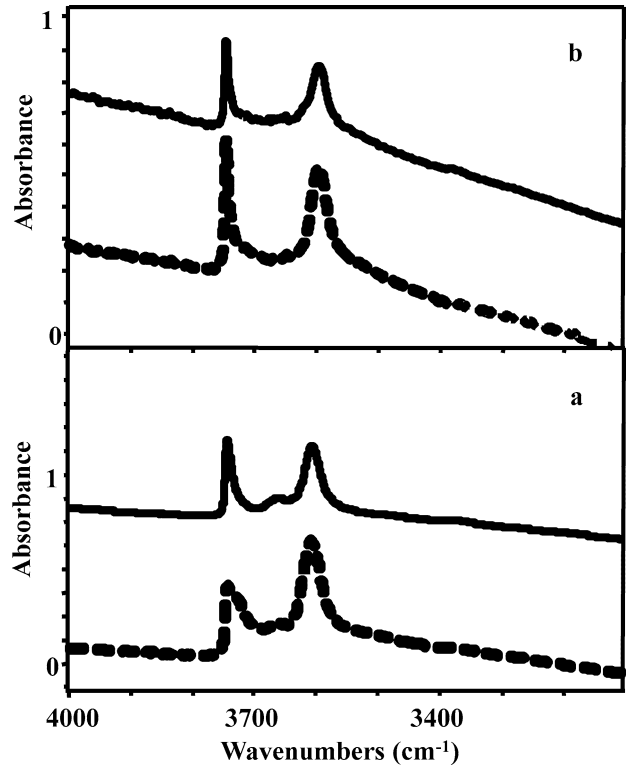

Fig. 4. FT-IR spectra in OHs stretching region of H-zeolites (···) and Co-exchanged zeolites (—) after outgassing at 773 K for 1 h: (a) MFI, (b) FER.

nor of $[Co^{2+}(OH)^{-}]^{+}$ species have been detected after outgassing.

3.3. IR studies

The IR spectra of the OH stretching bands of hydroxyl groups of activated Co-zeolites are compared to those of the corresponding H-zeolites in Fig. 4. As discussed elsewhere [23] the spectrum of H-FER shows a very sharp band at 3747 cm^{-1} which is due to the terminal silanol groups located on the external surface and weakly acidic; a broader band at 3600 cm^{-1} is due to the bridging Si–OH–Al groups that are exclusively on the inner surface and possess a strong Brønsted acidity. The Co-FER sample shows the same bands but with a loss of intensity. The absolute intensity of the band of the external silanol groups is near 70% for Co-H-FER with respect to the H-FER band, whereas the band of the internal bridging OHs is still 88% with respect to that of the unexchanged zeolite.

The spectra of Co-H-MFI and H-MFI samples show similar bands at 3747 and 3615 cm^{-1}, but with an additional weak band at 3660–3670 cm^{-1} that can be assigned to the OHs of extraframework species. Besides, H-MFI sample presents a component in the region 3730 cm^{-1} that is actually unusually strong [24–26]. We can calculate that 57% of the band due to terminal silanols and 50% of the band due to bridging OHs are still residual in the MFI exchanged sample.

We can note that, for bulk absorptions such as the skeletal vibrations in the region 1200–400 cm^{-1} and the overtones in the region 2200–1500 cm^{-1}, band intensities are just the same for Co-H-FER and H-FER and for Co-H-MFI and H-MFI. Thus, the intensity decrease of the OH bands is reasonably due to the disappearance of such bands due to the exchange of the protons for Co ions. Although a certain error (but probably small) can occur in this evaluation, we can conclude that for both Co-H-MFI and Co-H-FER, the exchange of protons is evidently only very partial, although more pronounced for MFI than for FER.

These data indicate that, in spite of the significant amount of cobalt loaded onto the zeolites and the absence of detectable Co-containing species other than those that exchanged for the protons, actually only a relatively small part of the bridging OHs underwent cation exchange. In particular, the large decrease of the band of the terminal silanols indicates that a significant part of cobalt ions actually exchanged for the OHs located at the external zeolite structure and are consequently thought to remain outside the channels.

To test whether the partial exchange with cobalt modified the acidity of the residual OHs and if the same Co sites are actually accessible, we investigated the adsorption of acetonitrile (AN) onto the catalyst surface (Figs. 5–7).

As previously reported [27], the adsorption of AN on H-FER and H-MFI surfaces perturbs the OH groups. The

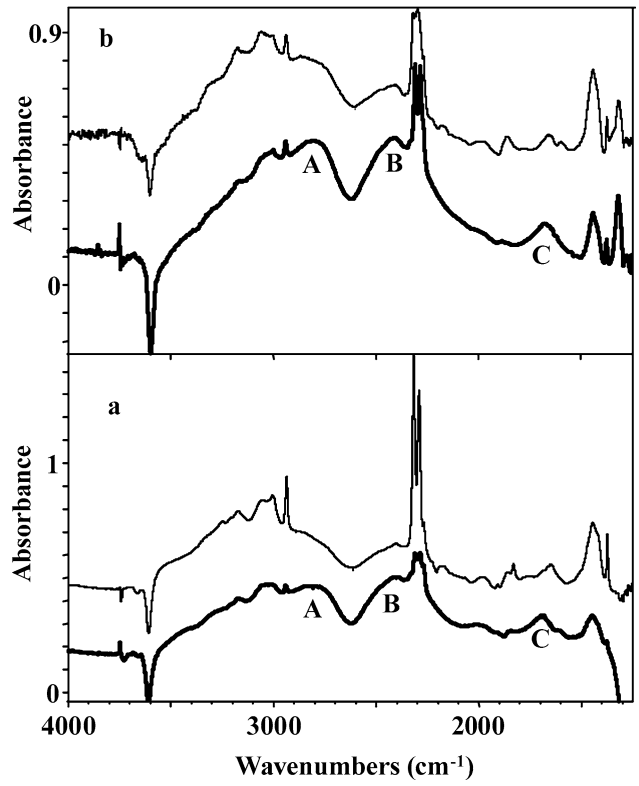

Fig. 5. FT-IR subtraction spectra (ABC pattern) of H-zeolites (—) and Co-exchanged zeolites (—) after AN adsorption and evacuation at rt; the spectra of activated samples have been subtracted. (a) FER, (b) MFI.

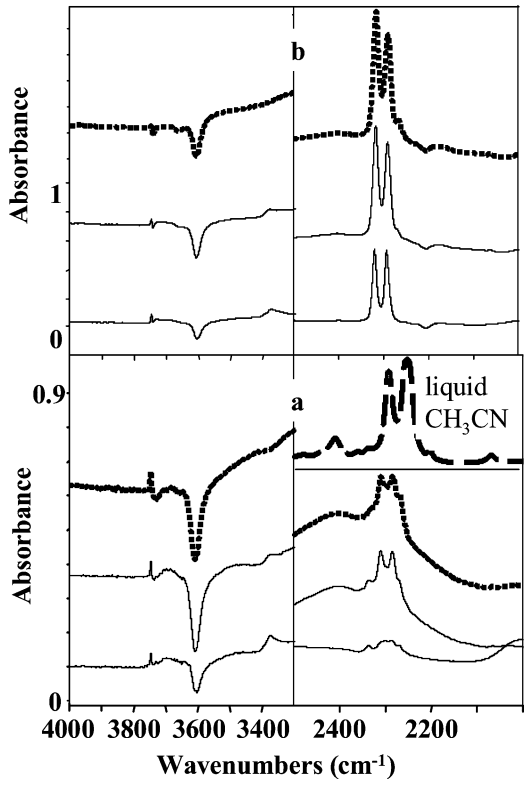

Fig. 6. FT-IR subtraction spectra of MFI samples (OH stretching region, left) after AN adsorption and evacuation, and of AN (–CN stretching region, right) adsorbed on catalyst surfaces. The spectra of the activated samples have been subtracted. (a) H-MFI, (b) Co-H-MFI; from the top: liquid AN (— —), evacuation at rt (···), at 373 K (—), and at 473 K (—), for 10 min.

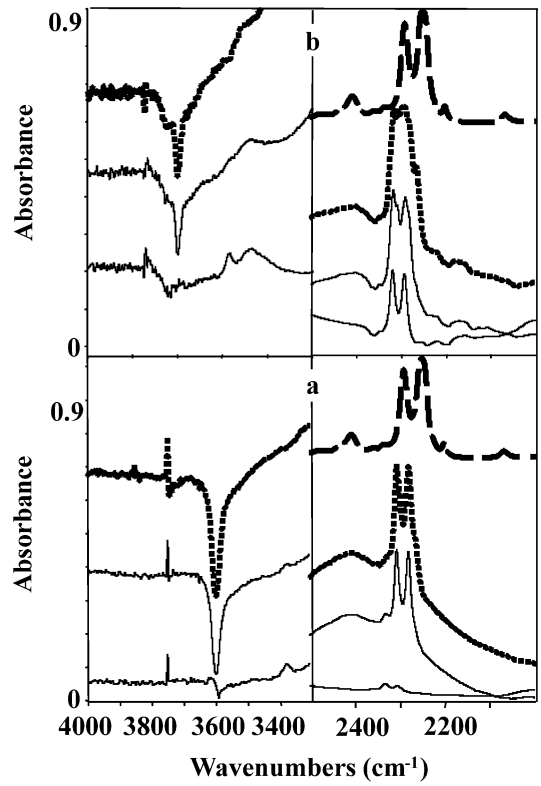

Fig. 7. FT-IR subtraction spectra of FER samples (OH stretching region, left) after AN adsorption and evacuation, and of AN (–CN stretching region, right) adsorbed on catalyst surfaces. The spectra of the activated samples have been subtracted. (a) H-FER, (b) Co-H-FER; from the top: liquid AN (— —), evacuation at rt (···), at 373 K (—), and at 473 K (—), for 10 min.

perturbation of the bridging hydroxyl groups, in particular, gives rise to the so called ABC pattern (Fig. 5): two intense and broad bands at around 2800 and 2400 cm^{-1}, a less intense one at around 1600 cm^{-1}, and a window with a minimum at around 2600 cm^{-1}, corresponding to $\sim 2\ \delta$OH. This so-called ABC pattern has been assigned to very strong quasi-symmetrical hydrogen bonding, where the proton is partially but not completely transferred to the base. It arises from the Fermi resonances between νOH and the overtones of δOH and γOH when the hydroxyl groups strongly interact with bases, as discussed elsewhere [28]. In Fig. 5 the results of subtraction of the spectra of activated zeolites from those obtained after adsorption of AN and evacuation at rt for 10 min, in order to eliminate the excess vapour phase, are shown. The ABC profiles of the Co–H-zeolites can be compared to those of H-zeolites. The addition of Co seems to determine a small (5–10 cm^{-1}) but significant shift down of the overall ABC spectrum. This should correspond to an increased average acidity of the residual hydroxyl groups, due either to a direct effect of Co^{2+} species on the acidity of the residual OHs or to an easier exchange of the most weakly acidic OHs. In any cases, the patterns of the exchanged samples are much less intense as a result of the partial disappearance of the bridging hydroxyl groups.

In Figs. 6 and 7, the spectra of adsorbed species arising from AN adsorption onto the catalysts are shown in the region 2600–2000 cm^{-1} (right side): the spectra of activated materials have been subtracted. Correspondingly, the subtraction spectra in the OH stretching region are shown (range 4000–3300 cm^{-1}, left side). For each zeolite the spectra collected after the evacuation steps at rt, 373 K, and 473 K are compared for exchanged and not-exchanged samples. Liquid acetonitrile shows a strong doublet at 2294 and 2254 cm^{-1}, the latter band being definitely stronger than the former. They are due to Fermi resonance between the –CN stretching and a $\delta CH_3 + \nu$C–C combination. This characteristic pattern changes when the –CN group adsorbs onto an acidic surface: the bigger the electron-withdrawal effect of either Brønsted or Lewis sites with which the N lone pair interacts the larger the shift upwards of the components and the inversion of their relative intensity, as previously reported [29].

In the case of AN adsorbed onto H-FER, a quite complex group of bands can be seen (Fig. 6a). For H-FER the doublet at 2307 and 2270 cm^{-1} is due to AN interacting with the bridging OHs and responsible for the ABC pattern. The further doublet at 2334 and 2307 cm^{-1} has been assigned to the AN interacting with extraframework or external Al Lewis sites, which are very strong acids. For H-MFI (Fig. 7a), the spectrum is more complex: here the interactions with Lewis sites are evidenced by a doublet at 2337 and 2299 cm^{-1} and, again, the main doublet is due

to H-bonded species (2309 and 2270 cm^{-1}). Actually, an additional component is observed at 2286 cm^{-1}.

The spectra of the Co-exchanged samples appear significantly different from those of the H-precursors and similar to each other (Figs. 6b and 7b). Both of them show a single doublet exactly at the same wavenumbers, 2319 and 2290 cm^{-1}, very strong in both cases, that resists outgassing at 473 K, characterised by a comparable intensity of the two components. This doublet is certainly due to AN interacting with the Co sites typical of the Co-exchanged zeolites. In principle, we cannot distinguish whether this cobalt actually is exchanging for the bridging OHs in the inner surface of the cavities or the external silanols. On the other hand both are likely similar, because on both the internal surface and the external one Co ions are nearly naked, oxide anions being substantially absent. The shape of these spectra seems to point out that Co species behave as medium-strong Lewis acidic sites.

To have even more information, we also investigated the adsorption of 2,2-dimethylpropionitrile (pivalonitrile) as a basic probe. In the case of Co-containing samples we found an adsorbed species characterized by a CN stretching band shifted to very high frequencies, up to above 2300 cm^{-1}, which is not found on protonic zeolites. Taking into account that this molecule does not enter the cavities of MFI and FER zeolites [29] it is evident that new Lewis sites, i.e., Co cations, are also located at the external surfaces of Co-containing zeolites, in agreement with the data arising from the OH stretching bands.

3.4. NH_3-TPD measurements

The surface acidity properties of the samples have also been investigated by the NH_3-TPD technique. The results of TPD measurements are reported in Figs. 8 and 9 and in Table 2. Only total amounts of desorbed NH_3 are calculated and reported in Table 2 because in many cases the overlapping of the peaks in TPD spectra makes their resolution arbitrary. In Fig. 8 the NH_3-TPD spectrum of Co-H-MFI is reported together with those of the parent H-MFI (NH_4-MFI activated at 823 K) and the reference Co_3O_4 oxide (supplied by Carlo Erba, 15 $m^2\,g^{-1}$). The spectrum of H-MFI shows two partially overlapping peaks at low temperature (379, 416 K) and a well-resolved peak at higher temperature (632 K). Similar TPD curves were reported for the H-MFI sample with comparable Si/Al ratio [30–33]. The low-temperature signals are supposed to be due to NH_3 hydrogen bonded to weak acid sites, probably silanol groups. The high-temperature signal is due to decomposition of NH_4^+ ions formed by interaction of NH_3 with zeolitic H^+ sites, as it is the only peak observed during deammoniation of NH_4^+–MFI. The Co-H-MFI sample also shows two TPD peaks at low-temperature followed by a high-temperature signal, similar to the parent H-MFI. However, the overall intensity is greatly increased (see also Table 2), and a broad unresolved additional component, likely centered at about 573 K, absent in the spectrum of the parent materials, appears. This shows the presence of Co species acting as medium-strong Lewis acid sites, in agreement with IR studies. It can be noted that the high-temperature signal, representative of protonated ammonia, is also present; by taking into account that this peak appears on the tail of a large signal, we can say that it is of lower intensity in comparison with the spectrum of the parent H-MFI. Therefore, we can deduce that a significant amount of H^+ sites are still present in the Co-zeolite. This agrees with the uncompleted Co exchange, evaluated by FT-IR measurements, notwithstanding that the Co amount is close to the theoretical exchange capacity. The peak due to NH_4^+ decomposition, in the case of Co-H-MFI, is shifted a little bit upwards, in agreement with a slightly increased acidity of the residual acid sites, as deduced from IR spectra, too.

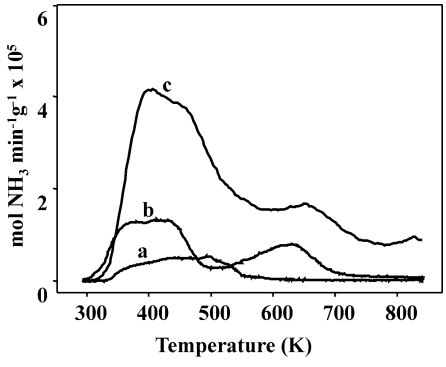

Fig. 8. NH_3-TPD curves of (a) Co_3O_4, (b) H-MFI activated at 773 K, (c) Co-H-MFI.

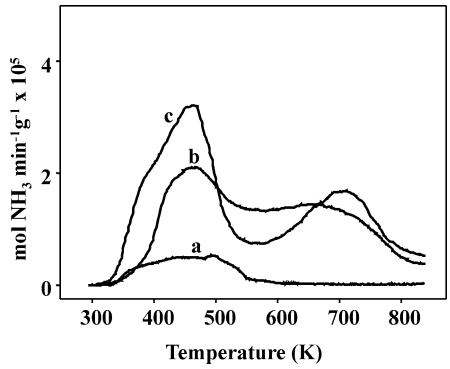

Fig. 9. NH_3-TPD curves of (a) Co_3O_4, (b) H-FER activated at 773 K, (c) Co-H-FER.

Table 2
NH_3 TPD results

	Total desorbed NH_3 (mmol g^{-1})	Peak temperature (K)
H-MFI	0.28	379, 416, 632
Co-H-MFI	1.00	406, 445, 654
H-FER	0.59	467, 674
Co-H-FER	0.72	467, 713
Co_3O_4	0.09	497

The NH_3-TPD spectrum of Co-H-FER is reported in Fig. 9, together with the spectra of the parent H-FER and of the reference Co_3O_4. Similarly to H-MFI and in agreement with literature data [34], the spectrum of H-FER shows a low-temperature signal due to hydrogen-bridge-bonded NH_3 and a high-temperature signal due to protonated NH_3. The spectrum of Co-exchanged zeolite shows a signal at 467 K, with a shoulder at about 383 K, and a well-resolved peak at 713 K. The high-temperature signal appears less broad and more regular and shifted to higher temperature in comparison to H-FER. The amount of ammonia adsorbed onto Co-H-FER is higher than that onto H-FER, suggesting the formation of new NH_3 adsorbing sites due to Co ions. The high-temperature peak is indicative, as observed for Co-H-MFI, of the presence of a large amount of residual H^+, suggesting that only a partial Co exchange took place. The shift of the maximum to higher temperature suggests an increase of the strength of protonic acid sites, as already observed in FT-IR spectra.

The amount of adsorbed ammonia in Co-H-zeolites (Table 2) indicates that two ammonia molecules can adsorb at each Co ion, and this amount adds to ammonia adsorbed on residual protons.

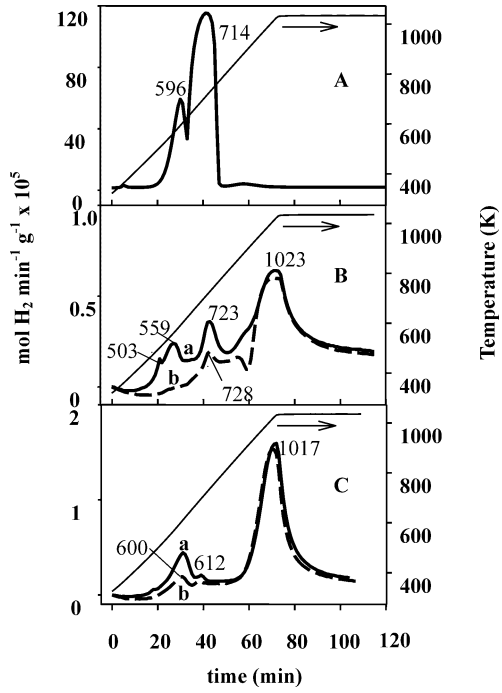

Fig. 10. H_2-TPR curves of (A) Co_3O_4 pretreated in air, (B) Co-H-MFI, and (C), Co-H-FER. (a) pretreatment in air, (b) pretreatment in He.

3.5. TPR analysis

The reducibility of Co sites in Co-exchanged zeolites has been studied by H_2-TPR. These measurements have been carried out on samples pretreated at 773 K either in air or in He flow. TPR measurements have also been performed on the parent zeolites and on the reference Co_3O_4, for comparison. The TPR profiles are compared in Figs. 10A–C, the amounts of consumed H_2, obtained from integration of TPR signals, are reported in Table 3. As expected, the original zeolites give no reduction signals. As shown in Fig. 10A, Co_3O_4 gives two TPR peaks at 596 and 714 K. The hydrogen consumption corresponding to the two reduction peaks (Table 3) is very close to the expected values for the two-step reduction: $Co^{3+} \rightarrow Co^{2+}$ and $Co^{2+} \rightarrow Co^0$. The spectrum of Co-H-MFI pretreated in air (Fig. 10B) shows three peaks at 559, 723, and 1023 K. For the sample pretreated in He we can notice that the first peak disappears while the second decreases in intensity and a peak at 820 K is evidenced. In contrast, the most intense peak at 1023 K is not influenced by the atmosphere of thermal treatment. This last signal cannot be attributed to Co oxide, since it is completely reduced at about 773 K (Fig. 10A). As suggested by Wang et al. [35], this signal can be attributed to Co^{2+} exchanging protons, which should be more resistant to reduction, because it is stabilised by the negatively charged zeolite framework. The intensity of the TPR peaks appearing at lower temperatures is affected by the treatment atmosphere (i.e., helium or air). This suggests that they are representative of reduction of cobalt oxide species that can easily change the oxidation state. The correspondence of the temperatures of such peaks to those of reduction of the Co_3O_4 phase seems to confirm this hypothesis. We can suppose that small amounts of easily reducible cobalt oxide phase, perhaps in nanosized particles, escaping the above characterisation techniques (FT-IR, UV–vis, XRD), have formed. An additional signal

Table 3
TPR results: peak temperatures, consumed H_2 amounts, and molar ratios H_2/Co

	Peak 1			Peak 2			Peak 3			Total	
Catalyst	T (K)	n_{H_2} [c]	H_2/Co	T (K)	n_{H_2} [c]	H_2/Co	T (K)	n_{H_2} [c]	H_2/Co	n_{H_2} [c]	H_2/Co
Co-H-MFI[a]	559	0.03	0.10	723	0.05	0.17	1023	0.23	0.80	0.31	1.0
Co-H-MFI[b]	–	–	–	728	0.05	0.17	1032	0.20	0.69	0.25	0.8
Co-H-FER[a]	594	0.06	0.15	–	–	–	1014	0.30	0.80	0.36	0.9
Co-H-FER[b]	612	0.04	0.10	–	–	–	1017	0.32	0.85	0.36	0.9
Co_3O_4[a]	596	4	0.32	714	12.5	1.00	–	–	–	16.5	1.32

[a] Pretreated in air.
[b] Pretreated in He.
[c] Consumed hydrogen, mmol g^{-1}.

is observed at somewhat lower temperature (503–563 K). Similar behaviour was reported by Jong and Chen [36] for Co-MFI prepared by impregnation. Taking into account the results obtained by Wang et al. [35], this signal can be attributed to the presence of polynuclear Co oxo-ions that are reduced to Co^0 nanoclusters by H_2. Such multinuclear ions can play an important role in adsorption and activation of NO_x species [35]. However, the same result can arise from a fraction of exchanged Co ions oxidized to the trivalent state.

The amount of consumed hydrogen per cobalt ion ranges from 0.8 to 1 (Table 3), thus being lower than the expected one for reduction of total cobalt, which includes exchanged Co^{2+} and cobalt oxide species. This could be due to a defective estimate of the high-temperature peak, since the reduction of exchanged Co^{2+} occurs at a slow rate and probably is not complete under isothermal conditions within the time of the tests.

The H_2-TPR profiles of Co-H-FER (Fig. 10C) are quite similar to those of Co-H-MFI. They show peaks at 594 K that can be attributed to easily reducible cobalt species, and the predominant one at 1014 K due to hardly reducible species. The intensity of low-temperature peaks is affected by the pretreatment atmosphere, while the high-temperature one is insensitive to pretreatment conditions. The dominant peak can be attributed again to reduction of exchanged Co^{2+} ions. The signals at 594 K is likely related to the presence of polynuclear Co oxo-ions, as observed for the Co-H-MFI sample. The somewhat higher peak temperature seems to indicate a lower reducibility of these species in comparison with Co-H-MFI. Moreover the signal in the range 673–723 K is very weak, suggesting the absence of a nanosized Co oxide phase, if any, different from the Co-H-MFI sample. The value of total H_2 consumption is lower than expected for reduction of all Co, probably due to very slow reduction of exchanged Co^{2+}.

3.6. Catalytic activity tests

The results of catalytic activity tests are reported in Figs. 11–14. In all tests the main products were CO_2, NO_2, and N_2 with trace amounts of CO. In no conditions was N_2O detected. In preliminary tests it was ascertained that no homogeneous NO oxidation to NO_2 occurred.

The NO and CH_4 conversions for Co-H-MFI and Co-H-FER are reported in Fig. 11 together with selectivity to N_2. Co-H-MFI appears more active than Co-H-FER in the whole temperature range. Both catalysts show a maximum in NO conversion, shifted to higher temperature for Co-H-FER. Selectivities to N_2 are increasing with temperature and exceed 50% only at high temperatures. This is due to the predominant formation of NO_2 at low temperature in agreement with previous data for Co-MFI catalysts [8,11]. By contrast, CH_4 conversion is always increasing with temperature, thus leading to a varying CH_4/NO reaction ratio: at temperatures lower than the maximum, this is close to or slightly higher than 1:2, while at higher temperatures it reaches

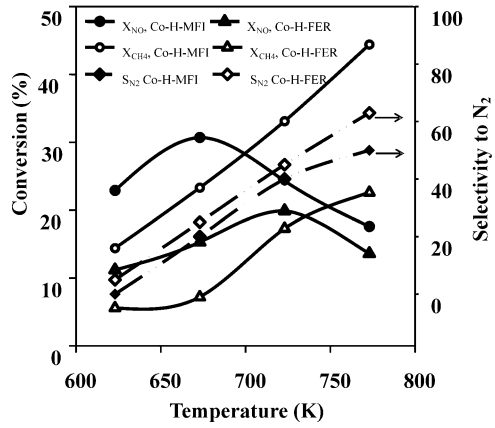

Fig. 11. NO and CH_4 conversion and selectivity to N_2 on Co-H-MFI and Co-H-FER. GHSV = 60,000 h^{-1}.

greatly exceeding values. This clearly suggests the occurrence of a side reaction also at high temperature, mainly methane combustion, as previously reported [6]. The occurrence of side reactions consuming CH_4 hardly explains the presence of maximum of NO conversion because methane is never limiting even at high temperature. The maximum in NO conversion is related to the occurrence of NO oxidation to NO_2, which predominantly occurs at low temperature but approaches equilibrium conversion at high temperature (see below), and gives rise to a decrease of NO conversion with temperature due to thermodynamics. For Co-H-FER the maximum of NO conversion is shifted to higher temperature probably because this catalyst is less active than Co-H-MFI also in NO oxidation catalysis, and thus shows the increase of NO conversion to NO_2 at higher temperature.

The catalytic behaviour of H-zeolites was also investigated. It can be observed that the not-exchanged zeolites show low activity, with maxima of NO conversion of about 10% at 650–700 K (GHSV = 60,000 h^{-1}) and decreasing values at higher temperatures. The samples are active mainly for NO oxidation to NO_2, which is practically the only reaction product at $T > 650$ K, and to a negligible extent towards NO reduction, in agreement with results reported elsewhere [33,37]. Similar behaviour was observed for H-FER.

The influence of GHSV on the most active catalyst, that is Co-H-MFI was investigated (Fig. 12). As expected, the increase of GHSV leads to a decrease of NO conversion, which reaches a maximum value of about 35% at 673 K. However, NO was converted mainly to NO_2, which was the main product at low temperature. As shown in Fig. 13, with increasing temperature, conversion to NO_2 decreases while conversion to N_2 increases and overcomes that to NO_2 at 773 K. These data clearly indicate a high activity of Co-H-MFI towards NO oxidation at low temperature.

In order to obtain more information about the catalyst activity towards this reaction, tests were carried out feeding NO and O_2 in the same concentrations as during CH_4-SCR tests, but in the absence of methane. The results are reported in Fig. 14, which also reports NO conversion to

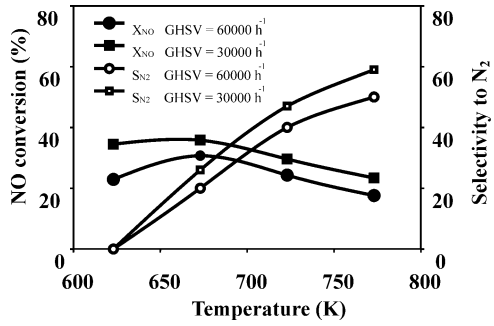

Fig. 12. NO conversion and selectivity to N_2 on Co-H-MFI at different GHSV.

NO_2 in equilibrium conditions. It can be observed that Co-H-MFI shows significant activity and that conversion to NO_2 reaches equilibrium values starting from 650 K. At $T \leqslant 650$ K conversion to NO_2 is practically the same as that observed in CH_4-SCR tests, while it is higher at higher temperatures. This suggests that under CH_4-SCR conditions NO_2 formation (prevailing at low temperature) can compete with the main reaction, giving rise to N_2; NO reduction by methane occurs only at higher temperatures where oxidation to NO_2 is thermodynamically limited. Similar results were reported by Cant and Liu for Co-MFI [11].

4. Discussion

The picture concerning the reaction mechanism upon CH_4-SCR is quite complex, and different authors came only to partial agreement. In particular, taking into account the papers published by Armor and co-workers [6,12], Cant and Liu [11], Kauchy et al. [8], Wang et al. [38], and Ivanova et al. [39], the following points about the reaction mechanism appear largely shared:

1. NO in the presence of O_2 is oxidized to an adsorbed NO_y species ($y = 2,\ 3$) and can also give rise to gaseous NO_2.
2. Methane is activated by adsorbed NO_y species *via* abstraction of a hydrogen atom.

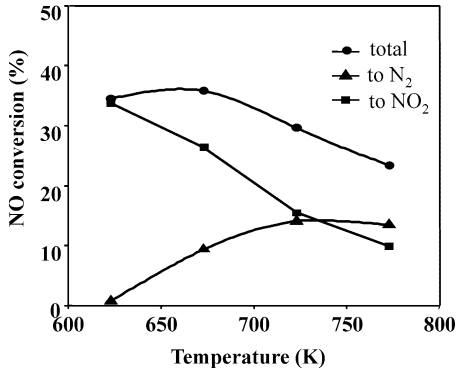

Fig. 13. Conversion of NO and conversion to N_2 and NO_2 on Co-H-MFI.

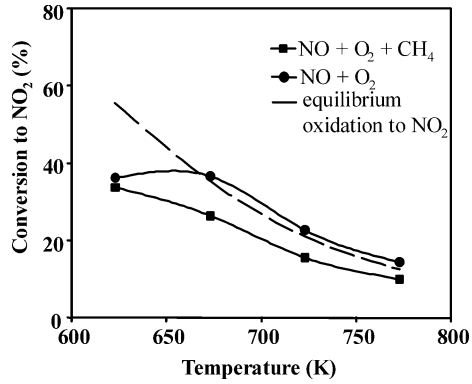

Fig. 14. NO oxidation to NO_2 on Co-H-MFI. GHSV = 30,000 h^{-1}.

3. A reactive intermediate containing C, H, N, and O (nitromethane- or nitrosomethane-like) is formed from the methyl group and an adsorbed NO_y species; this intermediate reacts with gaseous NO or NO_2, leading to the formation of the N_2 molecule.
4. Methane activation is the rate-determining step.

Otherwise, several different details are proposed by the different authors. In particular, disagreement can be found concerning the role of NO_2 either as a gaseous intermediate or only in the adsorbed state.

Different points of view are also reported in recent literature on the nature of active sites. Kauchy et al. [8] reported that exchanged Co sites (characterised as Co^{2+} [21]) exhibit activity in CH_4-SCR while protons or oxide-like Co species contribute to CH_4-SCR by enhancement of the oxidation of NO to NO_2. Wang et al. [38] point to the redox properties of catalysts and suppose that the activity of Co-MFI catalysts is due to the redox couple Co^{2+}/Co^0. Zerovalent Co species can be formed by reduction of Co polynuclear oxo-cations that appear easily reducible. According to Yan et al. [19] Co cations act in the oxidation of NO to NO_2 while Brønsted acid sites act in the true reduction step by methane.

Our own experimental data show that under CH_4-SCR conditions the following overall reactions can actually occur:

$$CH_4 + 2NO + O_2 \rightarrow N_2 + CO_2 + 2H_2O, \quad (2)$$

$$NO + \tfrac{1}{2}O_2 = NO_2, \quad (3)$$

$$CH_4 + 2O_2 \rightarrow CO_2 + 2H_2O. \quad (4)$$

At low temperatures reaction (3) is the main one over Co-H-zeolites. At high temperatures, when NO oxidation (3) is thermodynamically limited, reactions (2) and (4) become the prevailing ones. This suggests that NO_2 could not be a necessary intermediate in the CH_4-SCR reaction starting from NO; otherwise, its formation should be inhibited to have a good catalyst. The data we present here suggest that the mechanism is rake-type and that an intermediate NO_y (like that previously observed, e.g., by Ivanova et al. [38] for Co-zeolites, identified as a nitrate species) is likely

formed from NO and oxygen and can desorb as NO_2 (at low temperature when NO_2 is a stable compound) or as NO or react with methane, giving rise finally to N_2. This agrees, among other things, with the effect of space velocities towards selectivity to nitrogen upon CH_4-SCR (Fig. 12) and with the effect of methane on NO oxidation (Fig. 14). Interestingly, Co-H-FER, which is less active in converting NO to NO_2 at low temperature than Co-H-MFI, gives, however, higher selectivities to N_2.

Exchanged Co cations are certainly active in all three reactions (2)–(4). They have been characterized to be in the bivalent state in vacuum by UV–vis spectroscopy, in agreement with previous data [21], and this also agrees with their evident medium-strong Lewis acidity, found here both by IR of adsorbed acetonitrile and by TPD of adsorbed ammonia. TPR data obtained in the present work show that Co^{2+} ions exchanged in MFI and FER zeolites are reduced by hydrogen at about 1000 K; thus it is unlikely that such species can be reduced under the reaction conditions. On the other hand, far more easily reducible species are detected from TPR low-temperature signals. These species appear to be also easily oxidizable, since the TPR signals are clearly influenced by the atmosphere of thermal treatment. This suggests that a fraction of Co^{2+} ions, either those exchanging protons or a fraction which are clustered in nanosized oxide particles, are oxidized to Co^{3+} when treated in air at 773 K: the subsequent reduction of Co^{3+} to Co^{2+} in TPR measurement contributes to the low-temperature peaks. Thus, our data suggest that a Co^{2+}/Co^{3+} redox couple can be active for CH_4-SCR as well as for NO oxidation to NO_2. This couple is likely active also for methane and other alkane oxidation, as discussed previously for catalytic combustion over cobalt oxides [40,41].

Protonic zeolites are weakly active in NO oxidation to NO_2 and, even much less, for CH_4-SCR. On the other hand, the very acidic OHs of zeolites are well known to be active in adsorbing and perturbing hydrocarbon molecules [42] and nitrogen oxides as well, and can also act as methane combustion catalysts [43]. In particular, it is evident that hydrocarbons whose size allows penetration into the cavities tend to concentrate there, as reported elsewhere [42]. Our data indicate that the average Brønsted acidity of the residual bridging OHs is even a little increased with respect to nonexchanged protonic zeolites. It seems quite reasonable that the ability of these sites to adsorb both reactants can favor in more than one way the CH_4-SCR reaction. So the reported cooperating effect of Co and proton sites can be due to the enhanced rate of formation of the NO_y intermediate or to the enhanced rate of reaction of this intermediate with methane, whose concentration in the cavities is enhanced due to its interaction with the protons. In our opinion, this explains the cooperating effect of protons better than their weak activity in NO oxidation, although both things can occur to some extent.

Moreover, it must be considered that the sites, cobalt cations and protons, present on the external surface of zeolites could play a nonnegligible role in catalysis. Such a contribution, generally disregarded in the literature, is now under investigation.

5. Conclusions

Partially exchanged Co-H-FER and Co-H-MFI have been prepared and their properties characterised using different physicochemical techniques. Their catalytic activity towards CH_4-SCR and NO oxidation was studied under diluted conditions.

The main conclusions of this study can be summarized as follows:

- Partial Co exchange occurs with strong acid sites in the inner zeolitic cavities and also with weak silanol acidic groups on the external crystals surface; Co ions at the external zeolite surface are detected by IR, and could have a role in catalysis and in the spectroscopic behaviour in the UV–vis region.
- Both Co-H-FER and Co-H-MFI retain large amounts of residual protonic sites whose acid strength seems to be a little increased by the Co exchange; residual silanol groups are also found at the external zeolite surface.
- Cobalt ions act as medium-strength Lewis acid sites; TPR measurements give evidence that exchanged Co^{2+} ions are hardly reducible. However, a fraction of Co oxide species (either exchanged cations or polynuclear oxo-species) are easily reducible and oxidizable.
- Co-H-FER and Co-H-MFI zeolites are active both in NO selective catalytic reduction by methane and in the NO oxidation to NO_2. H-zeolites are weakly active, mainly for NO oxidation.
- NO oxidation to NO_2 competes with and prevails over CH_4-SCR when it is thermodynamically favoured, in the sense that NO_2 is formed instead of N_2. CH_4-SCR is predominant when NO oxidation to NO_2 is no more a favoured reaction.
- It is proposed that NO reduction occurs via a redox mechanism involving essentially a Co^{2+}/Co^{3+} redox couple and an NO_y adsorbed intermediate (possibly a nitrate species). This species can either give rise to NO_2 gas or react with methane.
- According to previous studies, it is proposed that protonic sites cooperate in CH_4-SCR mainly by adsorbing either NO (so favouring the formation of the intermediate) or methane (so favouring its reaction with the intermediate) or both.

Acknowledgments

The present work has been supported by the MICA (Italian Ministry of Industry, Trade and Handicraft) in the frame of Energy Research Program for the Italian Electrical

System (MICA Decree of January 26, 2000), Project on "Interaction between the electrical system and environment (SOSTE)."

References

[1] H. Bosch, F.J. Janssen, Catal. Today 2 (1988) 369.
[2] G. Busca, L. Lietti, G. Ramis, F. Berti, Appl. Catal. B 18 (1998) 1.
[3] Y. Li, J.N. Armor, Appl. Catal. B 1 (1992) L31.
[4] W. Held, A. Konig, T. Richter, L. Puppe, Soc. Aut. Eng., 1990, Paper 900496.
[5] M. Iwamoto, H. Yahiro, Y. Shundo, Y. Yu-u, N. Mizuno, Shokubai 32 (1990) 430.
[6] J.N. Armor, Catal. Today 26 (1995) 147.
[7] V. Indovina, M.C. Campa, S. De Rossi, G. Ferrarsi, Appl. Catal. B 8 (1996) 315.
[8] D. Kauchy, A. Vondrovà, J. Dedechek, B. Wichterlova, J. Catal. 194 (2000) 318.
[9] A.J. Desai, V.I. Kovalchuk, E.A. Lombardo, J.L. D'Itri, J. Catal. 184 (1999) 396.
[10] S.A. Beloshapkin, E.A. Paushktis, V.A. Sadykov, J. Mol. Catal. A Chem. 158 (2000) 355.
[11] N.W. Cant, I.O.Y. Liu, Catal. Today 63 (2000) 133.
[12] Y. Li, P.J. Battavio, J.N. Armor, J. Catal. 142 (1993) 561.
[13] M. Misono, CATTECH 2 (1998) 183.
[14] M. Shelef, Chem. Rev. 95 (1995) 209.
[15] P. Praserthdam, N. Mongkolsiri, P. Kanchanawanichkun, Catal. Commun. (2002), in press, available on the Internet.
[16] Z. Li, M. Flytzani-Stephanopoulos, Appl. Catal. B 22 (1999) 35.
[17] L. Gutierrez, A. Boix, J. Petunchi, Catal. Today 54 (1999) 451.
[18] L. Ren, T. Zhang, D. Liang, C. Xu, J. Tang, L. Lin, Appl. Catal. B 35 (2002) 317.
[19] J.-Y. Yan, H.H. Kung, W.M.H. Sachtler, M.C. Kung, J. Catal. 175 (1998) 294.
[20] W.M. Butler, C.L. Angell, W. McAllister, W.M. Risen, J. Phys. Chem. 81 (1977) 2061.
[21] D. Kauchy, J. Dedechek, B. Wichterlova, Micropor. Mesopor. Mater. 31 (1999) 75.
[22] J. Dedechek, D. Kauchy, B. Wichterlova, Micropor. Mesopor. Mater. 35–36 (2000) 483.
[23] M. Trombetta, G. Busca, M. Lenarda, L. Storaro, M. Pavan, Appl. Catal. A 182 (1999) 225.
[24] T. Armaroli, M. Trombetta, A. Gutièrrez Alejandre, J. Ramirez Solis, G. Busca, Phys. Chem. Chem. Phys. 2 (2000) 3341.
[25] R.M. Dessau, K.D. Schmitt, G.T. Kerr, G.L. Woolery, L.B. Alemany, J. Catal. 104 (1987) 484.
[26] A. Zecchina, S. Bordiga, G. Spoto, L. Marchese, G. Petrini, G. Leofanti, M. Padovan, J. Phys. Chem. 88 (1992) 2959.
[27] M. Trombetta, G. Busca, J. Catal. 187 (1999) 521.
[28] A.G. Pelmenschikov, G.H.M.C. van Wolput, J. Jänchen, R.A. van Santen, J. Phys. Chem. 99 (1995) 3612;
A.G. Pelmenschikov, R.A. van Santen, J. Phys. Chem. 97 (1993) 10678.
[29] G. Busca, Phys. Chem. Chem. Phys. 1 (1999) 723.
[30] H. Ichibashi, M. Kitamura, Catal. Today 73 (2002) 23.
[31] R.Q. Long, R.T. Yang, J. Catal. 198 (2001) 20.
[32] F. Lonyi, J. Valyon, Micropor. Mesopor. Mater. 47 (2001) 293.
[33] F.G. Requejo, J.M. Ramallo-Lopez, E.J. Lede, E.E. Miró, L.B. Pierella, O.A. Annunziata, Catal. Today 54 (1999) 553.
[34] P. Cañizares, A. Carrero, P. Sànchez, Appl. Catal. A 190 (2000) 93.
[35] X. Wang, H. Chen, W.M.H. Sachtler, Appl. Catal. B 29 (2001) 47.
[36] S. Cheng, S.-J. Jong, Appl. Catal. A 126 (1995) 51.
[37] E. Kikuchi, M. Ogura, N. Aratani, Y. Sugiura, S. Hiromoto, K. Yogo, Catal. Today 27 (1996) 35.
[38] X. Wang, H.Y. Chen, W.M.H. Sachtler, J. Catal. 197 (2001) 281.
[39] E. Ivanova, K. Hadjiivanov, D. Klissurski, M. Bevilacqua, T. Armaroli, G. Busca, Micropor. Mesopor. Mater. 46 (2001) 299.
[40] E. Finocchio, G. Busca, V. Lorenzelli, V. Sanchez Escribano, J. Chem. Soc. Faraday Trans. 92 (1996) 1587.
[41] G. Busca, V. Lorenzelli, G. Ramis, V. Sanchez Escribano, in: L. Guczi, F. Solymosi, P. Tetenyi (Eds.), New Frontiers in Catalysis, Elsevier, Amsterdam, 1993, pp. 2661–2664.
[42] T. Armaroli, M. Trombetta, A. Gutièrrez Alejandre, J. Ramirez Solis, G. Busca, Phys. Chem. Chem. Phys. 2 (2000) 3341.
[43] J.R. Anderson, P. Tsai, Appl. Catal. 19 (1985) 141.